MNRAS **000**, 1–9 (2019) Preprint 6 February 2022 Compiled using MNRAS LATEX style file v3.0

Revisiting the statistical isotropy of GRB sky distribution

Uendert Andrade,[1]★ Carlos A. P. Bengaly,[2]† Jailson S. Alcaniz,[1,3]‡
Salvatore Capozziello[4,5,6,7]§

[1] *Observatório Nacional, Rio de Janeiro, RJ 20921-400, Brasil*
[2] *Department of Physics & Astronomy, University of the Western Cape, 7535 Cape Town, South Africa,*
[3] *Departamento de Física, Universidade Federal do Rio Grande do Norte, Natal, RN 59072-970, Brasil,*
[4] *Dipartimento di Fisica "E. Pancini", Università di Napoli "Federico II",*
Complesso Universitario di Monte Sant' Angelo, Edificio G, Via Cinthia, I-80126, Napoli, Italy.
[5] *Istituto Nazionale di Fisica Nucleare (INFN), Sezione di Napoli,*
Complesso Universitario di Monte Sant'Angelo, Edificio G, Via Cinthia, I-80126, Napoli, Italy.
[6] *Gran Sasso Science Institute, viale F. Crispi 7, I-67100, L'Aquila, Italy.*
[7] *Laboratory for Theoretical Cosmology,*
Tomsk State University of Control Systems and Radioelectronics (TUSUR), 634050 Tomsk, Russia.

arXiv:1905.08864v2 [astro-ph.CO] 14 Oct 2019

Accepted XXX. Received YYY; in original form ZZZ

ABSTRACT

The assumption of homogeneity and isotropy on large scales is one of the main hypotheses of the standard cosmology. In this paper, we test the hypothesis of isotropy from the two-point angular correlation function of 2626 gamma-ray bursts (GRB) of the FERMI GRB catalogue. We show that the uncertainties in the GRB positions induce spurious anisotropic signals in their sky distribution. However, when such uncertainties are taken into account no significant evidence against the large-scale statistical isotropy is found. This result remains valid even for the sky distribution of short-lived GRB, contrarily to previous reports.

Key words: Large-scale structure of Universe – methods: data analysis – gamma-ray burst: general

1 INTRODUCTION

One of the foundations of modern cosmology is the so-called Cosmological Principle (CP), which consists in the assumption that the Universe looks homogeneous and isotropic on large scales. Statistical analyses using recent cosmological observations bring evidence that the CP holds true at such scales, as obtained from the Cosmic Microwave Background (CMB) temperature anisotropies (Ade et al. 2016), cosmic distances from type Ia Supernovae (Andrade et al. 2018b; Deng & Wei 2018; Sun & Wang 2018; Andrade et al. 2018a; Zhao et al. 2019; Soltis et al. 2019), galaxy number counts (Gibelyou & Huterer 2012; Yoon et al. 2014; Bengaly et al. 2018a; Rameez et al. 2018), the sky distribution of galaxy clusters (Bengaly et al. 2017; Migkas & Reiprich 2018). There is also evidence for a homogeneity scale in the counts of quasars and galaxies (Scrimgeour et al. 2012; Ntelis et al. 2017; Gonçalves et al. 2018a,b). However, some controversial claims have appeared in the literature, such as large-angle features in the CMB (Schwarz et al. 2016) and a large dipole anisotropy in radio source counts (Singal 2011; Rubart & Schwarz 2013; Bengaly et al. 2018b) (see also Dolfi et al. 2019.).

Gamma-ray bursts (GRB) have also been used to test the CP. These events are extremely energetic explosions, whose range lies between $10^{50} - 10^{54}$ erg, which exceeds hundred times the total energy radiated by a supernova. Also if they are not properly *standard candles*, they may reveal themselves as possible formidable distance indicators. For a detailed discussion on the topic, we refer the reader to Amati & Della Valle 2013; Dainotti & Amati 2018; Dainotti et al. 2018. They are usually classified into short-lived ($T_{90} < 2s$, SGRBs) and long-lived ($T_{90} > 2s$, LGRBs), where T_{90} denotes the duration in which 90% of the burst fluence is accumulated. The LGRBs have been thought to originate from distance star-forming galaxies and associated with collapse of massive stars related to a supernova (SN). However, LGRBs with no clear association with any bright SN have been found. Besides, some LGRBs were observed in a very metal-rich systems, in contradiction to the core-collapse model (Woosley & Bloom 2006). Hence, the forma-

★ E-mail: uendertandrade@on.br
† E-mail: carlosap87@gmail.com
‡ E-mail: alcaniz@on.br
§ E-mail: capozziello@na.infn.it

© 2019 The Authors

tion of LGRBs besides the collapse scheme is still a mater of debate. SGRBs are attributed to mergers between neutron star-black hole (NS-BH) or NS-NS. However, Perna et al. (2016) proposed an alternative scenario that can also lead to a SGRB from mergers of BH-BH. Therefore, SGRBs have been correlated with the local Universe (Tanvir et al. 2005; Ghirlanda et al. 2006), while LGRBs typicall consist of higher redshift objects, $z \sim 9.4$ (Cucchiara et al. 2011).

In the last decades, several authors have shown that the GRBs sky distribution is consistent with statistical isotropy (Hartmann & Blumenthal 1989; Hartmann et al. 1991; Meegan et al. 1992; Briggs et al. 1996; Tegmark et al. 1996). However, subsequent works suggested otherwise for SGRBs (Balazs et al. 1998; Meszaros et al. 2000; Magliocchetti et al. 2003; Vavrek et al. 2008; Tarnopolski 2017). Moreover, there are also claims for the existence of GRB structures of $\sim$ 2000 Mpc at $z \sim 2$ (Horvath et al. 2014, 2015; Ruggeri & Capozziello 2016) – for a different conclusion, see also (Bernui et al. 2008; Gibelyou & Huterer 2012; Li & Lin 2015; Ukwatta & Wozniak 2016; Tarnopolski 2017; Ripa & Shafieloo 2017, 2018)[1].

Given the relevance of the topic, and the current controversies, we revisit in this paper the question of the statistical isotropy in the GRB sky distribution. The analysis performed uses the two-point angular correlation function (2pACF) of 2627 gamma-ray bursts of the Fermi Gamma-ray Burst Monitor Burst catalogue. We show that, after removing objects with large sky positional errors, there is no evidence of anisotropy signatures for the whole GRB sample, as well as for LGRBs and SGRBs sub-samples. We also applied our data analysis to the Burst And Transient Source Experiment (BATSE) current GRB catalogue of the Compton Gamma Ray Observatory (CGRO) satellite containing 2702 GRBs and similar results are found.

This paper is organised as follows. In Sec. II the observational data set used in the analysis is discussed. The methodology and data analysis performed are presented in Sec. III. Sec. IV presents our main results whereas Sec. V discusses such results and summarises our main conclusions.

2 THE OBSERVATIONAL DATA SET

In our analysis we use the Fermi Gamma-ray Burst Monitor Burst Catalogue, termed FERMIGBRST (Gruber et al. 2014; von Kienlin et al. 2014; Bhat et al. 2016). This catalogue is one of the most complete GRB catalogues currently available, comprising 2627 objects detected from July 14th 2008 until August 06th 2019 [2]. Specifically, we make use of the following quantities:

(i) RA: The Right Ascension of the burst, given in J2000 decimal degree.
(ii) DEC: The Declination of the burst, given in J2000 decimal degree.
(iii) ErrorRadius: The uncertainty of the object position, in degrees. We term it as σ_r, which ranges from zero, when the source localisation was obtained using something other than Fermi GBM (for example, Swift, XMM), up to $\sim 68°$.
(iv) T_{90}: The duration, in seconds, during which 90% of the burst fluence was accumulated.

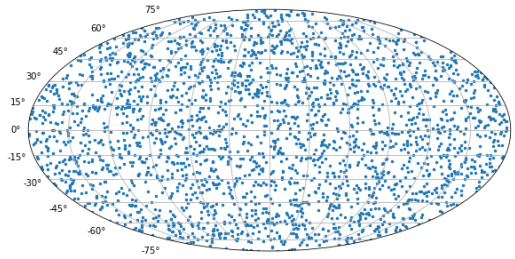


Figure 1. Mollweide projection of the GRB sky positions of the FERMIGBRST catalogue.

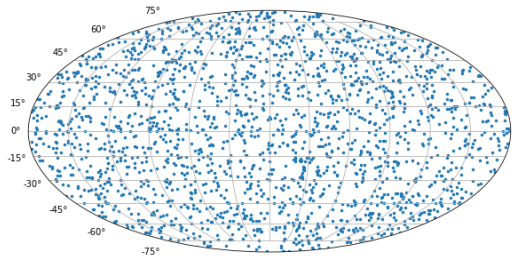


Figure 2. The same as Fig. 1, but for the CGRO/BATSE catalogue

For completeness, we also use the BATSE current Gamma-Ray Burst catalogue, which contains 2702 GRBs detected from March 21th 1991 until May 26th 2000[3]. We make use of similar quantities as the FERMIGRBST catalogue.

The FERMIGRBST and CGRO/BATSE sky distribution of the selected GRBs are displayed in the Fig. 1 and Fig. 2, respectively. Note that we removed one object in the former and 665 objects in the latter, because they do not contain information on the T_{90} parameter. We test the statistical isotropy for three cases, namely the whole GRB sample, (allGRB), as well as the LGRB and SGRB sub-samples.

3 DATA ANALYSIS

3.1 Two-point angular correlation function

In order to summarise the distribution of data points in the sky, one can report the mean number of points at a given scale. However, in the presence of clustering, the mean may be an insufficient descriptor, as this measure is insensitive to it. The 2pACF is a statistic capable of characterising the clustering of objects in the sky, which we denote by $\omega(\theta)$.

[1] In addition to test the CP, GRB have also been used to probe fundamental physics (Petitjean et al. 2016).
[2] https://heasarc.gsfc.nasa.gov/W3Browse/fermi/fermigbrst.html.
[3] https://heasarc.gsfc.nasa.gov/W3Browse/all/batsegrb.html.

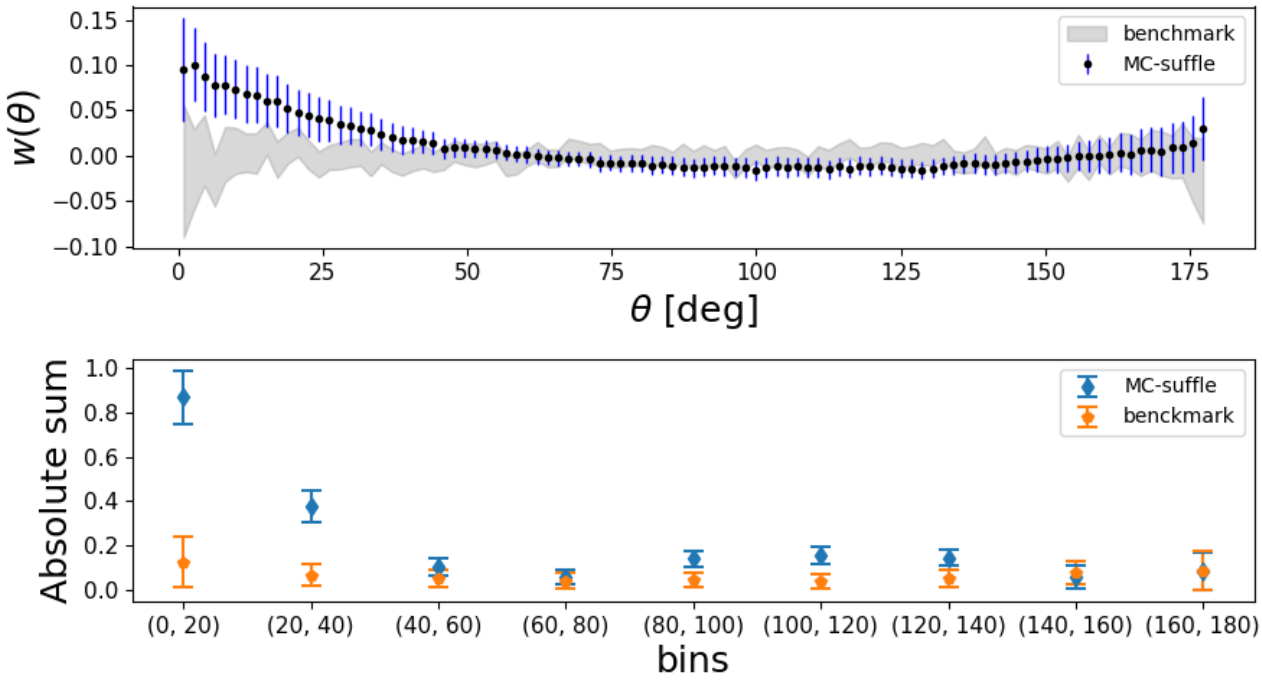


Figure 3. *Top*: Comparison between the 2pACF of the MC-shuffle realisations and the benchmark ones. Blue dots represent the former, while shaded regions correspond to the latter within the standard deviation bounds. *Bottom*: The absolute sum test. These results were obtained assuming 20° size bin, and $\sigma_r \leq 20°$.

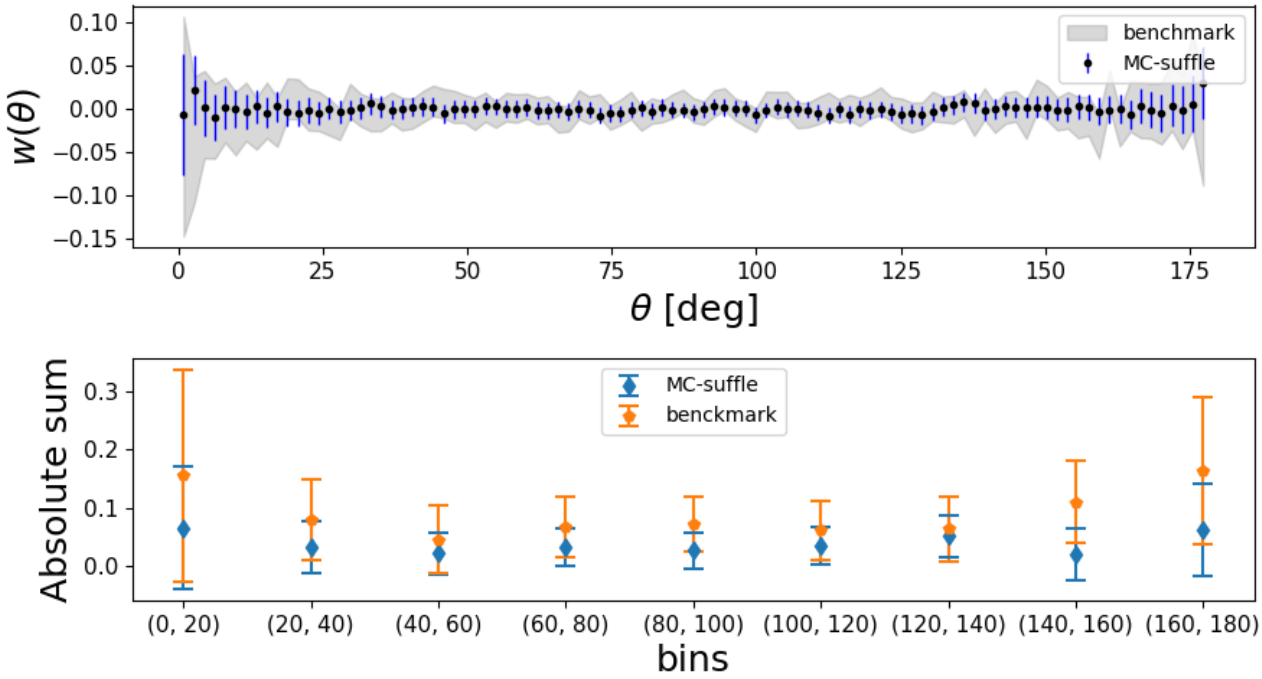


Figure 4. The same as Fig. 3, but valid for $\sigma_r \leq 6°$.

Essentially, it provides the probability to find a pair of object encompassed in a given solid angle with respect to an isotropic distribution (Peebles 1980). As a result, the 2pACF is null in the absence of clustering, and it is statistically similar for all angular scales if the underlying distribution is statistically isotropic.

We can determine the 2pACF from the data using the well-known Landy-Szalay estimator (Landy & Szalay 1993),

$$\omega(\theta) = \frac{\langle DD(\theta)\rangle - 2\langle DR(\theta)\rangle + \langle RR(\theta)\rangle}{\langle RR(\theta)\rangle}, \quad (1)$$

where the brackets denote the normalised number of all GRB pairs in the real data ($DD(\theta)$), in the auxiliary random isotropic catalogue ($RR(\theta)$), and between the data and the random catalogue ($DR(\theta)$). The counts of pairs for each angular scale is carried out through the range $(\theta - d\theta/2, \theta + d\theta/2)$, where $d\theta$ is the bin width. We choose evenly spaced samples in our analysis, so that $\omega(\theta)$ is calculated over the interval $(0°, 180°)$ with $d\theta = 1.8°$. The random isotropic catalogues are generated following a uniform distribution on a sphere, so that

$$\mathrm{RA} = 0° + (360° - 0°)\, U[0,1), \quad (2)$$

$$\mathrm{DEC} = \arcsin\left(-90° + (180°)\, U[0,1)\right). \quad (3)$$

We estimate our uncertainties of the 2pACF via bootstrap method (Tarnopolski 2017). By means of 100 resamplings between the data and the random catalogue, we obtain a bootstrap sampling distribution of the 2pACF whose uncertainty is the standard deviation of this sampling distribution. We also compute the 2pACF for isotropic random sample through Monte Carlo (MC) method, and perform the bootstrap analysis on it as well. We denote the mean and the standard deviation of this distribution as the *benchmark* (Tarnopolski 2017), since it provides the 2pACF limits that a finite isotropic sample must satisfy. Any significant deviation from this benchmark would hint at departures from statistical isotropy.

3.2 Absolute sum test

In order to further investigate the readability of the anisotropic signal, we devised what we hereafter call "Absolute sum test". We defined it as the summation of the absolute 2pACF values within a specific angular scale, i.e.,

$$\text{Absolute sum} \equiv \sum_i |\omega(\theta)|_i \ \forall i \in \Delta\theta, \quad (4)$$

where $\Delta\theta$ is the angular range at which we split the $\omega(\theta)$, so that we perform this summation in a tomographic fashion within this range, i.e., $i_1 = (0°, 20°), i_2 = (20°, 40°), \ldots, i_9 = (160°, 180°)$. We choose $\Delta\theta = 20°$ in order to have at least 10 values of $\omega(\theta)$ within this interval (since $d\theta = 1.8°$) and thus a robust statistics for each i-bin. Hence we can compare the 2pACF at different angular scales for two distributions, e.g. the real data versus the benchmark. Again, any deviation beside the error bars (as obtained from standard uncertainty propagation) suggests potential deviations from statistical isotropy, after all, the 2pACF values should agree at different angular if this assumption holds.

3.3 Statistical significance estimate

We assess the statistical significance of our analysis by means of non-parametric tests between two different samples as follows:

(i) Kolmogorov-Smirnov (KS): It consists of a distribution-free test which compares the empirical cumulative distribution function (ECDF) of two samples (Ivezić et al. 2014). This test relies on a metric which measures the maximum distance of the two ECDF $F_m(x)$ and $G_n(x)$,

$$D = \max |F_\mathrm{m}(x) - G_\mathrm{m}(x)| \,. \quad (5)$$

(ii) Anderson-Darling (AD): This test is based on the following statistics (Scholz & Stephens 1987):

$$A^2_\mathrm{mn} = \frac{mn}{N} \int_{-\infty}^{\infty} \frac{\{F_\mathrm{m}(x) - G_\mathrm{n}(x)\}^2}{H_\mathrm{N}(x)\{1 - H_\mathrm{N}(x)\}} dH_\mathrm{N}(x) \,. \quad (6)$$

F_m and G_n are ECDF for two independent samples that may have different number of points, namely n and m, respectively. $H_\mathrm{N}(x) = \{mF_\mathrm{m} + nG_\mathrm{n}\}/N$ is the ECDF of the pooled sample, where $N = m + n$.

Our null hypothesis is that the two sample are drawn from the *same* distribution. KS test is sensitive to the location, the scale and the shape of the distribution, while AD test is only sensitive to the shape. Moreover, AD test is more sensitive to the tails differences than KS test, which in turn is more sensitive to the differences near the centre of the distribution. In this sense, these two non-parametric tests are complementary.

We choose $\alpha = 0.05$ as the significance level in which we reject the null hypothesis. Hence, a p-value *lower* than α when we compare the real data with the benchmark, for example, would denote that the samples are not drawn from the same distribution - and thus the data is not statistically isotropic. We used the routines KS_2SAMP and ANDERSON_KSAMP of the SciPy Python library to compute the KS and AD statistics, as well as the p-values[4].

3.4 GRB positional uncertainties

Previous works showed that the GRB positional uncertainties might affect the measurement of the 2pACF and angular power spectrum of their celestial distribution (Hartmann et al. 1991; Tegmark et al. 1996). Here, in order to investigate the impact of such uncertainties on our analysis, we produce 1000 Monte Carlo (MC) realisations with the following prescription:

$$\mathrm{RA}_\mathrm{new} = \mathcal{N}\left(\mathrm{RA}, \sigma_\mathrm{r}^2\right); \quad (7)$$

$$\mathrm{DEC}_\mathrm{new} = \mathcal{N}\left(\mathrm{DEC}, \sigma_\mathrm{r}^2\right). \quad (8)$$

Due to the shuffling of GRB celestial positions, we henceforth call this test *MC-shuffle*. We compute the 2pACF for each of these realisations, then we take their mean and

[4] Jones E, Oliphant E, Peterson P, et al. SciPy: Open Source Scientific Tools for Python, 2001-, http://www.scipy.org/ [Online; accessed 2018-11-13].

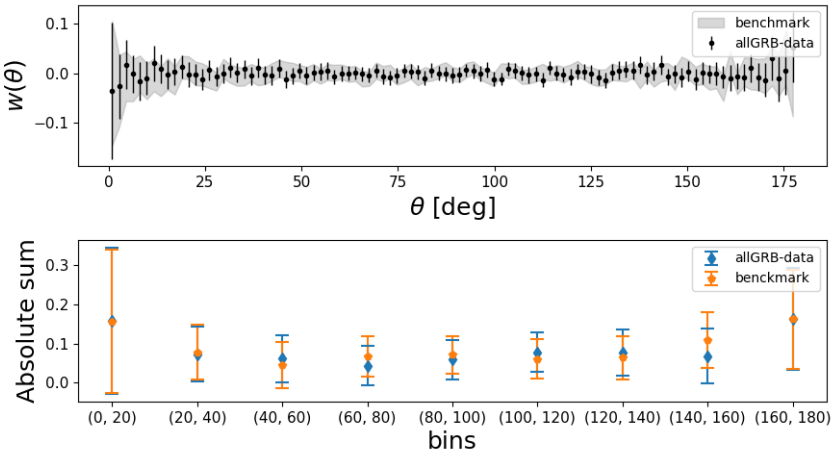


Figure 5. *Top*: The 2pACF obtained from a synthetic isotropic sample (benchmark; shaded regions), and from the GRBs FERMIGBRST catalogue with $\sigma_r \leq 6°$ (black dots). *Bottom*: The absolute sum of the 2pACF per bin, again with bin size. The diamond markers correspond to the real data, while pentagon markers represent the isotropic realisations. These results are valid for the FERMIGBRST allGRB sample.

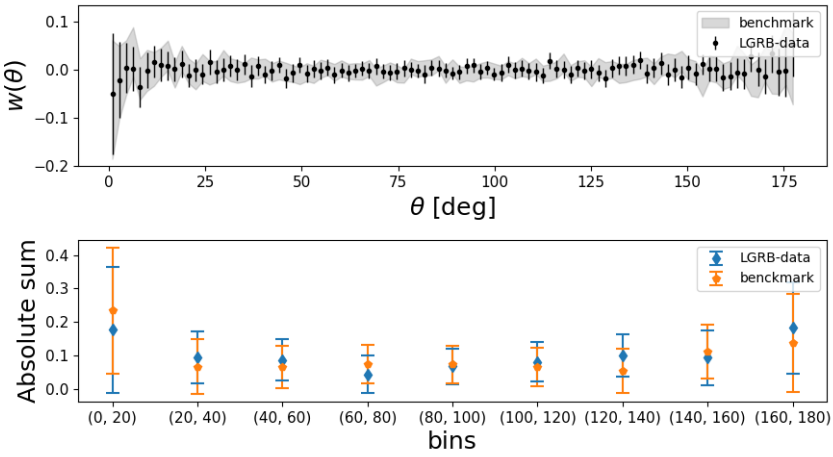


Figure 6. The same as Fig. 5, but for FERMIGBRST LGRB sample.

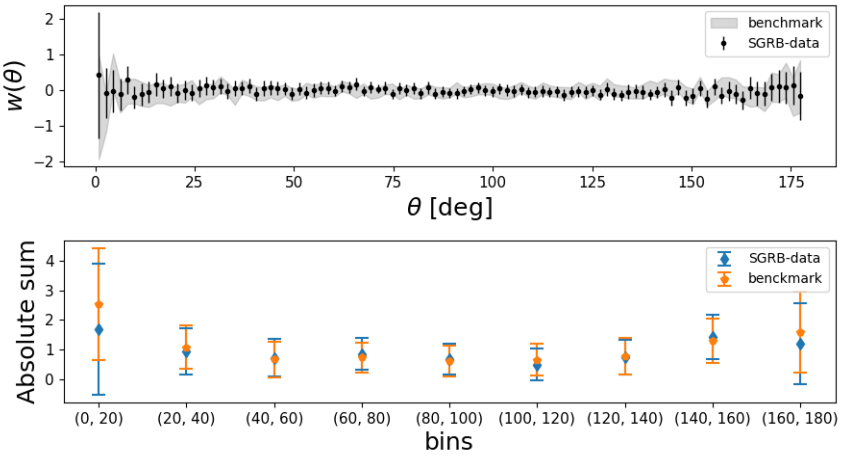


Figure 7. The same as Fig. 5, but for FERMIGBRST SGRB sample.

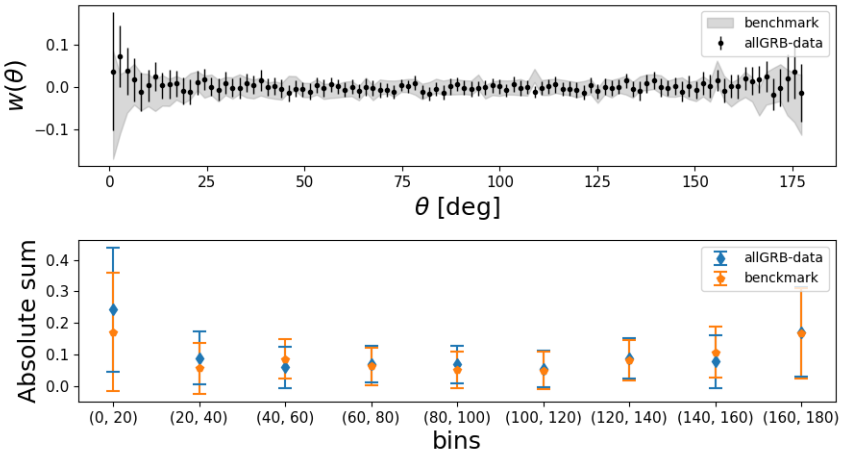


Figure 8. The same as Fig. 5, but for the CGRO/BATSE allGRB sample.

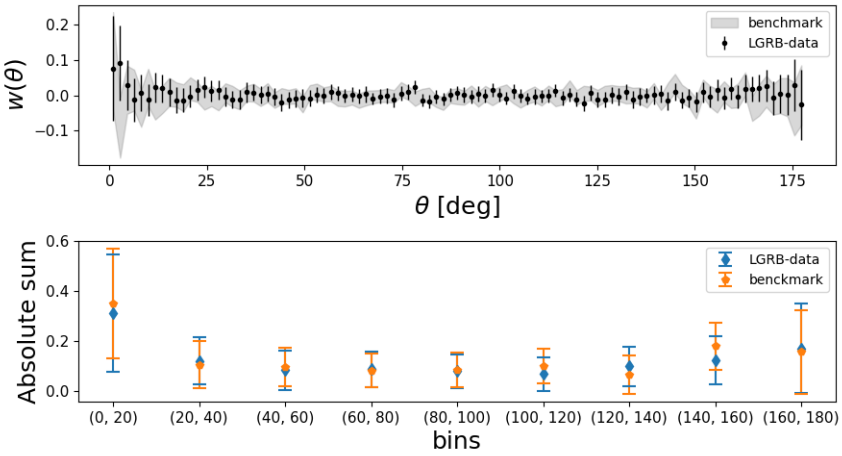


Figure 9. The same as Fig. 8, but for CGRO/BATSE LGRBs

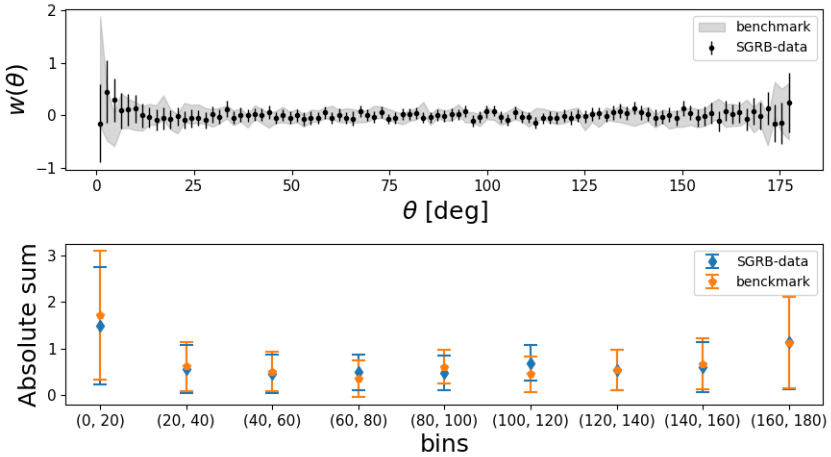


Figure 10. The same as Fig. 8, but for CGRO/BATSE SGRBs

standard deviation, and compare them with the benchmark. We repeat this procedure for different positional uncertainty cutoffs, which we denote by σ_r. If we find significant discrepancy between these MC-shuffle and benchmark realisations for less restrictive cutoffs, this will hint at spurious anisotropies arising due to such uncertainties.

4 RESULTS

We depict the impact of GRB positional errors on the 2pACFs in Fig. 3 and Fig. 4. By comparing the MC-shuffle and the benchmark with an upper limit of $\sigma_r = 20°$ and $\sigma_r = 6°$, we can clearly see that the latter is in better agreement with the benchmark, especially on smaller angular scales. This result shows that large positional errors indeed introduce spurious anisotropic signatures, as previously reported in Hartmann et al. (1991); Tegmark et al. (1996), and therefore we should impose an upper σ_r cutoff in our working sample. The GRB sub-sample with $\sigma_r \leq 6°$ will be hereafter taken as our real data sample, since it alleviates this feature, and we do not lose a large fractional of GRB, as we still retain 1760 GRBs in total, i.e., 1590 LGRBs and 170 SGRBs.

We compare the 2pACF between the real data and the benchmark in the upper panels of Fig. 5, while the bottom ones display the results from the absolute sum test as described in Section 3.2. The results obtained for LGRBs and SGRBs samples are displayed, respectively, in Fig. 6 and 7. Once more the shaded regions in the upper panels provide the allowed region which an intrinsic isotropic sample can vary due to randomness. From theses plots, we can conclude that both the 2pACF and the absolute sum show a good agreement between the allGRBs, LGRBs and SGRBs and the benchmark, and therefore no evidence against statistical isotropy. We verified that our results are unchanged for sub-samples of GRBs with fluence above a given value as 5×10^{-6} erg cm^{-2} or 10^{-5} erg cm^{-2}

In addition, we show the results obtained from the non-parametric tests in Table 1. We obtain that we cannot reject the null hypothesis at significance level of $\alpha = 0.05$ for all data samples, including SGRBs, although they yield the lowest p-value among all. We then confirm that the sky distribution of FERMIGBRST catalogue of GRBs is statistically isotropic, as expected from the CP.

For completeness, we also report the same analysis for the CGRO/BATSE GRB catalogue in Figs. 8, 9 and 10 for the allGRBs, LGRBs and SGRBs, respectively. We follow Chen & Hakkila (1998) who found that sky-exposure effects are small and should not affect our results. Here again, we see an agreement with the benchmark, which means no departure from statistical isotropy. The non-parametric tests for the CGRO/BATSE data set are displayed in Table 2. Although this set shows consistency with statistical isotropy, the allGRB sample shows departure from isotorpy. We discuss this latter result in the next section.

[5] Negative values of AD statistic means that the p-value was obtained as an upper limits and the true value might be larger than 0.25

Table 1. Results using both the Kolmogorov-Smirnov statistic D and the Anderson-Darling statistic AD for the FERMIGBRST catalogue.

	allGRBs	LGRBs	SGRBs
D	0.11	0.11	0.14
p-value	0.55	0.55	0.26
AD	-0.36[5]	-0.88	0.37
p-value	≥0.25	≥ 0.25	0.24

Table 2. Results using both the Kolmogorov-Smirnov statistic D and the Anderson-Darling statistic AD for the CGRO/BATSE catalogue.

	allGRBs	LGRBs	SGRBs
D	0.21	0.11	0.12
p-value	0.02	0.55	0.44
AD	4.3	0.17	-0.24
p-value	0.006	≥ 0.25	≥ 0.25

5 DISCUSSION AND CONCLUSION

One of the major concepts of modern cosmology is the assumption of the statistical homogeneity and isotropy on large scales. Together with the Einstein's field equations, they are at the basis of what we know as modern cosmology.

In this paper, we probed the statistical isotropic hypothesis of the CP by means of the 2pACF of the GRB sky distribution. To perform our analysis, we compared the 2pACF of the Fermi GRB catalogue with the 2pACF of the isotropic synthetic sample. We also investigated how the uncertainty in the GRBs position might affect ours conclusion by drawing 1000 MC simulations with new GRB positions inside the radius of the observational positional uncertainty.

We found that large positional uncertainties lead to spurious anisotropy detection, as shown in Fig. 3. For this reason, we perform cuts on the position uncertainty, choosing $\sigma_r = 6°$ as an optimal upper cut in which we can avoid spurious anisotropy without losing too many sources. Then, we split the data in three samples: all GRBs, LGRBs and SGRBs, containing 1760, 1590 and 170 each, respectively, after this cutoff. Fig. 5, 6, and 7 show the results for each sample, respectively. We found a good agreement between all these data and the statistical isotropy hypothesis, since the 2pACF and the absolute sum test agrees with the benchmark simulations. This was also confirmed by the KS and AD tests between the real data and the benchmark, whose p-values are shown in Table 1. None of these p-values were smaller than 0.05, meaning we cannot reject the null hypothesis at this significance level. We remark that in the case of SGRB, despite a lower p-value, one still cannot reject the null hypothesis.

We performed the same analysis for the CGRO/BATSE GRB catalogue, whose results are shown in Fig. 8, 9 and 10 for allGRB, LGRB and SGRB samples, respectively, as well as in Table 2. We conclude that statistical isotropy holds in this catalogue as well, although that the allGRB sample exhibits a stronger departure from this assumption. We credit this anisotropy to the impact of the sky-exposure function.

Although Chen & Hakkila (1998) showed that the effect on the 2pACF is small using a simple χ^2 analysis, we argue that our analysis is more sensitive, and thus we could capture the impact of the sky-exposure function in the 2pACF as other anisotropy tests e.g. dipole and quadrupole moments (Meegan et al. 1996). This result shows that our method is robust enough to capture even small anisotropy effects.

We conclude that there is no significant evidence for isotropy departure in the currently available GRB catalogues - even in the the SGRB sub-samples. This result is in good agreement with Tarnopolski (2017); Ukwatta & Wozniak (2016); Ripa & Shafieloo (2017, 2018), although we used an updated sample of GRB, and a different estimator. Therefore, we confirm the validity of statistical isotropy of the GRB distribution across the sky, which should be definitely underpinned in light of forthcoming Gamma-Ray surveys like e.g. THESEUS (Amati et al. 2018). Specifically, this space mission is aimed to exploit GRBs in view of investigating the early Universe and then providing a substantial advance in time-domain astrophysics. Due to the wide range of redshift that this mission can reach, it can also be extremely interesting for multi-messenger astrophysics as well.

ACKNOWLEDGEMENTS

U.A. acknowledges financial support from CAPES. C.A.P.B. acknowledges financial support from the South African SKA Project. J.S.A. acknowledges support from CNPq (grant Nos. 310790/2014-0 and 400471/2014-0) and FAPERJ (grant No. E-26/203.024/2017). S.C. acknowledges support from INFN (*Iniziativa Specifica* QGSKY) and CANTATA COST action CA15117.

REFERENCES

Ade P. A. R., et al., 2016, Astron. Astrophys., 594, A16
Amati L., Della Valle M., 2013, International Journal of Modern Physics D, 22, 1330028
Amati L., et al., 2018, Adv. Space Res., 62, 191
Andrade U., Bengaly C. A. P., Santos B., Alcaniz J. S., 2018a, Astrophys. J., 865, 119
Andrade U., Bengaly C. A. P., Alcaniz J. S., Santos B., 2018b, Phys. Rev., D97, 083518
Balazs L. G., Meszaros A., Horvath I., 1998, Astron. Astrophys., 339, 1
Bengaly C. A. P., Bernui A., Alcaniz J. S., Ferreira I. S., 2017, Mon. Not. Roy. Astron. Soc., 466, 2799
Bengaly C. A. P., Novaes C. P., Xavier H. S., Bilicki M., Bernui A., Alcaniz J. S., 2018a, Mon. Not. Roy. Astron. Soc., 475, L106
Bengaly C. A. P., Maartens R., Santos M. G., 2018b, JCAP, 1804, 031
Bernui A., Ferreira I. S., Wuensche C. A., 2008, Astrophys. J., 673, 968
Bhat P. N., et al., 2016, Astrophys. J. Suppl., 223, 28
Briggs M. S., et al., 1996, Astrophys. J., 459, 40
Chen X., Hakkila J., 1998, in AIP Conference Proceedings. pp 149–153
Cucchiara A., et al., 2011, ApJ, 736, 7
Dainotti M. G., Amati L., 2018, PASP, 130, 051001
Dainotti M., Del Vecchio R., Tarnopolski M., 2018, Adv. Astron., 2018, 4969503
Deng H.-K., Wei H., 2018, Eur. Phys. J., C78, 755
Dolfi A., Branchini E., Bilicki M., Balaguera-Antolínez A., Prandoni I., Pandit R., 2019, Astron. Astrophys., 623, A148
Ghirlanda G., Magliocchetti M., Ghisellini G., Guzzo L., 2006, Mon. Not. Roy. Astron. Soc., 368, L20
Gibelyou C., Huterer D., 2012, Mon. Not. Roy. Astron. Soc., 427, 1994
Gonçalves R. S., Carvalho G. C., Bengaly C. A. P., Carvalho J. C., Bernui A., Alcaniz J. S., Maartens R., 2018a, Mon. Not. Roy. Astron. Soc., 475, L20
Gonçalves R. S., Carvalho G. C., Bengaly C. A. P., Carvalho J. C., Alcaniz J. S., 2018b, Mon. Not. Roy. Astron. Soc., 481, 5270
Gruber D., et al., 2014, Astrophys. J. Suppl., 211, 12
Hartmann D., Blumenthal G. R., 1989, Astrophys. J., 342, 521
Hartmann D., Linder E. V., Blumenthal G. R., 1991, Astrophys. J., 367, 186
Horvath I., Hakkila J., Bagoly Z., 2014, Astron. Astrophys., 561, L12
Horvath I., Bagoly Z., Hakkila J., Toth L. V., 2015, Astron. Astrophys., 584, A48
Ivezić Ž., Connolly A., Vanderplas J., Gray A., 2014, Statistics, Data Mining and Machine Learning in Astronomy. Princeton University Press
Landy S. D., Szalay A. S., 1993, Astrophys. J., 412, 64
Li M.-H., Lin H.-N., 2015, Astron. Astrophys., 582, A111
Magliocchetti M., Ghirlanda G., Celotti A., 2003, Mon. Not. Roy. Astron. Soc., 343, 255
Meegan C. A., Fishman G. J., Wilson R. B., Paciesas W. S., Pendleton G. N., Horack J. M., Brock M. N., Kouveiotou C., 1992, Nature, 355, 143
Meegan C. A., et al., 1996, ApJS, 106, 65
Meszaros A., Bagoly Z., Horvath I., Balazs L. G., Vavrek R., 2000, Astrophys. J., 539, 98
Migkas K., Reiprich T. H., 2018, Astron. Astrophys., 611, A50
Ntelis P., et al., 2017, JCAP, 1706, 019
Peebles P. J. E., 1980, The large-scale structure of the universe. Princeton University Press
Perna R., Lazzati D., Giacomazzo B., 2016, Astrophys. J., 821, L18
Petitjean P., Wang F. Y., Wu X. F., Wei J. J., 2016, Space Sci. Rev., 202, 195
Rameez M., Mohayaee R., Sarkar S., Colin J., 2018, Mon. Not. Roy. Astron. Soc., 477, 1772
Ripa J., Shafieloo A., 2017, Astrophys. J., 851, 15
Ripa J., Shafieloo A., 2018, Arxiv:1809.03973
Rubart M., Schwarz D. J., 2013, Astron. Astrophys., 555, A117
Ruggeri A. C., Capozziello S., 2016, Astrophys. Space Sci., 361, 279
Scholz F. W., Stephens M. A., 1987, Journal of the American Statistical Association, 82, 918
Schwarz D. J., Copi C. J., Huterer D., Starkman G. D., 2016, Class. Quant. Grav., 33, 184001
Scrimgeour M., et al., 2012, Mon. Not. Roy. Astron. Soc., 425, 116
Singal A. K., 2011, Astrophys. J., 742, L23
Soltis J., Farahi A., Huterer D., Liberato C. M., 2019, Phys. Rev. Lett., 122, 091301
Sun Z. Q., Wang F. Y., 2018, Mon. Not. Roy. Astron. Soc., 478, 5153
Tanvir N., Chapman R., Levan A., Priddey R., 2005, Nature, 438, 991
Tarnopolski M., 2017, Mon. Not. Roy. Astron. Soc., 472, 4819
Tegmark M., Hartmann D. H., Briggs M. S., Meegan C. A., 1996, Astrophys. J., 468, 214
Ukwatta T. N., Wozniak P. R., 2016, Mon. Not. Roy. Astron. Soc., 455, 703
Vavrek R., Balazs L. G., Meszaros A., Horvath I., Bagoly Z., 2008, Mon. Not. Roy. Astron. Soc., 391, 1741
Woosley S. E., Bloom J. S., 2006, Ann. Rev. Astron. Astrophys.,

44, 507
Yoon M., Huterer D., Gibelyou C., Kovács A., Szapudi I., 2014, Mon. Not. Roy. Astron. Soc., 445, L60
Zhao D., Zhou Y., Chang Z., 2019, Arxiv:1903.12401
von Kienlin A., et al., 2014, Astrophys. J. Suppl., 211, 13

This paper has been typeset from a TEX/LATEX file prepared by the author.